

We are IntechOpen, the world's leading publisher of Open Access books Built by scientists, for scientists

6,900

Open access books available

186,000

International authors and editors

200M

Downloads

Our authors are among the

154

Countries delivered to

TOP 1%

most cited scientists

12.2%

Contributors from top 500 universities



WEB OF SCIENCE™

Selection of our books indexed in the Book Citation Index
in Web of Science™ Core Collection (BKCI)

Interested in publishing with us?
Contact book.department@intechopen.com

Numbers displayed above are based on latest data collected.
For more information visit www.intechopen.com



Fusion Welding with Indirect Electric Arc

Rafael García¹, Víctor-Hugo López¹, Constantino Natividad²,
Ricardo-Rafael Ambriz³ and Melchor Salazar⁴

¹*Instituto de Investigaciones Metalúrgicas-UMSNH,*

²*Facultad de Química-UNAM*

³*Instituto Politécnico Nacional CIITEC-IPN,*

⁴*Instituto Mexicano del Petróleo*

México

1. Introduction

The indirect electric arc technique (IEA) is a welding process that was initially developed to weld aluminum metal matrix composites (MMCs) reinforced with high content of TiC particles. Later on, its use was extended to weld MMCs reinforced with low contents of SiC and Al₂O₃ particles and monolithic materials such as carbon steels, aluminum and aluminum alloys. This technique is based on using the gas metal arc welding process (GMAW). In this instance, however, fusion of the base metal is not realized by the direct contact between the electric arc and the work pieces. Instead, the application of the electric arc is on thin plates of feeding metal placed on top of the work pieces and aligned with the groove of the joint. The filler wire, fed in a spray transfer mode, forms a weld pool with the plates of feeding metal and the molten metal is instantaneously fed, at high temperature, into the groove of the joint. The heat input supplied with the molten metal melts the side walls of the work pieces enabling welding upon solidification. The IEA technique allows using feeding material with the same chemical composition of the base metal. It has been found that the microstructure obtained in the weld metal with this technique, in carbon steels, improves the resistance to stress corrosion in hydrogen sulfide. The IEA technique has proved to be effective in welding MMCs with low and high content of ceramic particles, aluminum and its alloys as well as carbon steels such as API X-65 employed for transport and storage of hydrocarbons.

The design of the IEA joint enables welding of plates, 12.5 mm thick, in a single welding pass with a reduced heat input and thereby a reduction in the thermal affection of the base metal. Trials to weld materials such as aluminum and MMCs with a thickness of 12.5 mm in one welding pass without joint preparation, i.e. square edges, resulted in deficient welds with partial penetration. Successful welding of these plates demands 3 or 4 welding passes using a single V joint design. Conversely, the use of the IEA technique with preheating of the joint led to welds with full penetration and without lack of fusion in the side walls in a sole welding pass. The multipass welding procedure required for the single V groove joint means a larger heat input which inevitably has an impact on the microstructure of the different regions of the welded joint and of course on its mechanical performance. A thermal balance of the IEA process revealed a larger thermal efficiency as compared to the

traditional use of the GMAW welding process. This increase is ascribed to the fact that the electric arc is not openly exposed to the atmosphere. Instead, it is established in a hidden fashion within the groove formed by the feeding plates, reducing thus heat losses. This characteristic of the IEA technique has outstanding repercussions on the microstructure and mechanical properties of the welds. For example, degradation of the reinforcement during fusion welding of aluminum matrix composites reinforced with SiC particles is a common occurrence. Welding of this type of MMC with IEA did not show signs of reaction and a larger fraction of SiC particles were incorporated into the weld metal increasing the tensile properties of the welded joint. Also, in carbon steels, aluminum and its alloys the use of the IEA leads to a different solidification mode and grain refined microstructures. In particular, for an API X-65 this refinement has a profound positive effect in terms of sulfide stress cracking (SSC) behavior. Regarding heat treatable aluminum alloys, it is well known the overaging effect in the heat affected zone (HAZ) which weakens the strength of the alloy and predisposes failure in this region with a very low stress. The reduced heat input of the IEA technique also reduces the loss of strength in the HAZ of this type of alloys.

The main disadvantage of the IEA technique is that it leaves the residual feeding plates on top of the welded joint. This would be unacceptable in most of the applications. Thus, an additional step in the process demands removing these strips from the weld. To overcome this inconvenient, a modification of the design of the IEA joint was proposed and tested in heat treatable aluminum alloys. The use of the strips of feeding material on top of the work pieces was omitted and in the upper part of the work pieces a lash was machined, simulating the original feeding plates. The modified indirect electric arc (MIEA) technique drew similar results than the original IEA and when compared with the conventional single V groove joint, the behavior of the MIEA welds was better in both static and dynamic testing.

So far, the IEA technique and its evolution into the MIEA has emerged as an attractive alternative to weld a number of materials with peculiar microstructural characteristics that have a positive impact in the mechanical and stress corrosion cracking (SCC) behaviors. This chapter details a broad description of the process, emphasizing its advantages with respect to the conventional practice of fusion welding. An overview of the findings and benefits observed in different materials as well as the evolution of the original idea throughout ten years of research are provided.

2. Overview of the IEA welding process

The indirect electric arc (IEA) technique is a novel welding process that has been successfully used to join MMCs (Garcia et al, 2002a, 2002b, 2003). It is a variation of the metal inert gas (MIG) process in which fusion of the base metal is not caused by direct contact with the electric arc. Instead, the electric arc is established between the filler metal and feed metal, in plate form, placed over the base metal (Fig. 1), where the feed metal plates, base metal and filler metal all have similar chemical compositions. The plates are prepared with square edges and with a small single-V preparation with an angle of 45° in the upper part. The IEA technique allows using feeding material with the same chemical composition. The resultant droplets, in the form of a spray, produce a molten pool on the plates and the liquid is fed instantaneously at high temperature into the groove formed between the workpieces (Lu & Kou, 1989a, 1989b). The high temperature of the liquid metal melts the parent materials, producing the welded joint. Due to the increase of the thermal efficiency of the IEA process, complete penetration

and uniform weld beads, in a single pass, were obtained, as well as a reduction in the heat input and thereby a reduction in the thermal affection of the base metal compared with that provoked by the direct application of the electric arc (Garcia et al., 2002a, 2002b, 2003).

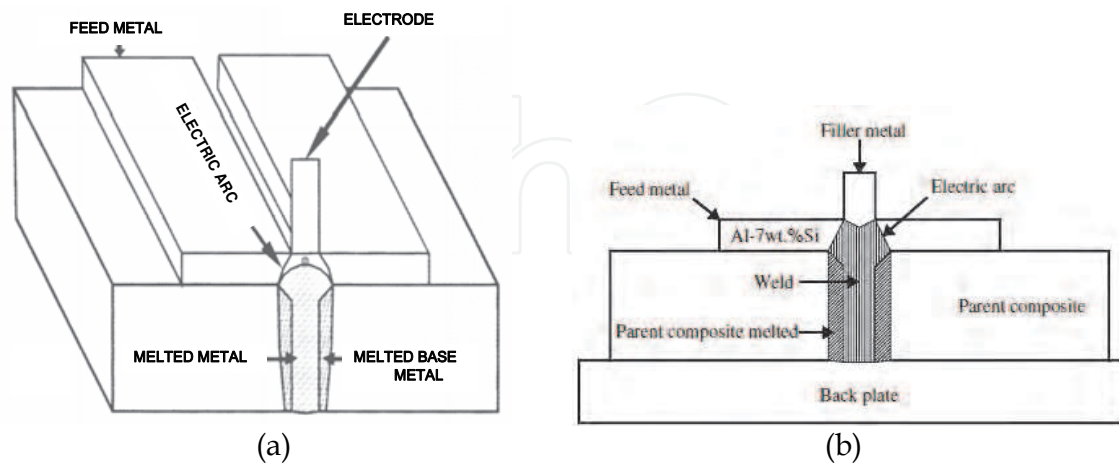


Fig. 1. IEA welding process: (a) General set-up (Garcia et al., 2002); (b) Set-up for application to 359 aluminum MMCs reinforced with 20%SiC (Garcia et al., 2007).

The fusion process of the base material is carried out by means of a liquid diffusion process, similar that the shown in Fig. 2a, where the liquid material diffuses through the grain boundaries, because these are areas of lower melting point than the matrix of the grains. This phenomenon is favored due to segregation of impurities and alloying elements in metals of high purity and alloying elements in alloys, respectively. Fig. 2b-c illustrates the difference between the indirect electric arc and the traditional electric arc welding processes. In the majority of the electric arc welding processes, the electric arc is established between the electrode and the base metal. The high energy developed by the electric arc is in direct contact with base metal and the forces generated in the weld pool affect the weld form and solidification mode. As illustrated in Fig. 2b, the temperature gradient within the weld pool induces a corresponding density gradient that enhances the flow and generates radial forces (RF) and circular forces (CF). Fig. 2b shows that when materials of a higher temperature and lower density are moving toward the bottom of the puddle, the buoyancy forces tend to rise up the liquid flow across the center of the pool. The flow moves radially outward, the molten metal is forced along the surface and then down the side of the weld pool toward the bottom (Domey et al., 1995). In the IEA technique, the electric arc is established within the feeding plates and as soon as the filler metal and feed metal are melted, liquid metal with low density is supplied into the joint geometry at high temperature. Thus, in the IEA process the buoyancy-driven flow is interrupted due to the presence of a deep groove and as a result, the radial forces instead of becoming circular forces, are transformed into "drag forces", a combined effect of the pressure exerted by the electric arc and the gravity action, drives the molten pool downwards into the groove formed by the workpieces, as can be seen in Fig. 2c. In addition, the hidden arc in the IEA method suggests that the loss of energy by radiation is suppressed and as a consequence, the efficiency of the electric arc in melting the feed metal is increased.

Along with the stir forces generated in the weld pool, the extent of supercooling also accounts for the mode of solidification. Although there are some exceptions, in electric arc welding epitaxial growth is a typical occurrence, wherein the first grains of the weld pool

nucleate directly from randomly oriented grains in the HAZ and grow toward the greatest thermal gradient within the puddle (Domey et al., 1995). On the other hand, the solidification in the IEA welding method is different due to the distinct generation of forces and flow patterns in the weld pool. Fusion of the base metal is realized by the high energy of the melt supplied into the joint geometry. The improvement of the efficiency of the MIG welding process to about 95% using IEA may be ascribed to the better use of heat generated by the electric arc, which is established in a hidden form and the contact with the environment is minimum reducing thus heat losses.

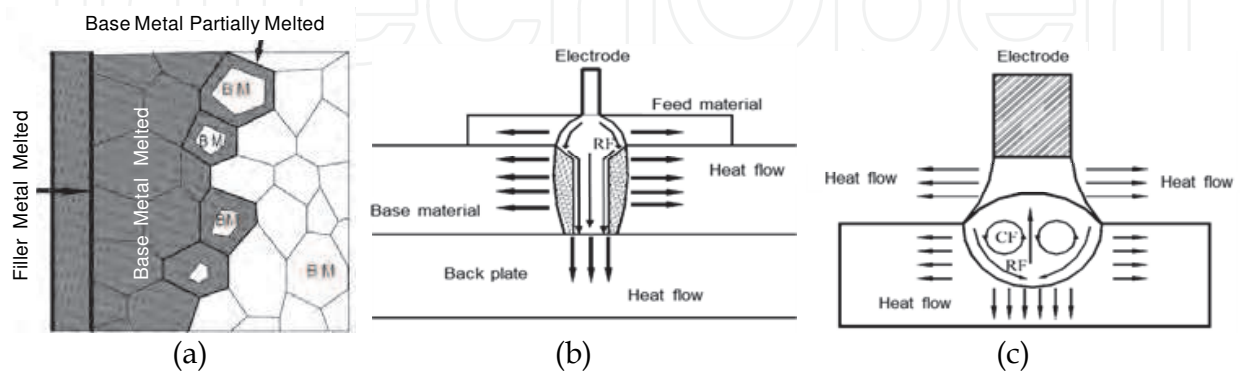


Fig. 2. (a) Fusion process by liquid diffusion; Schematic of the MIG welding process using (b) direct electric arc and (c) indirect electric arc (Garcia et. al, 2002).

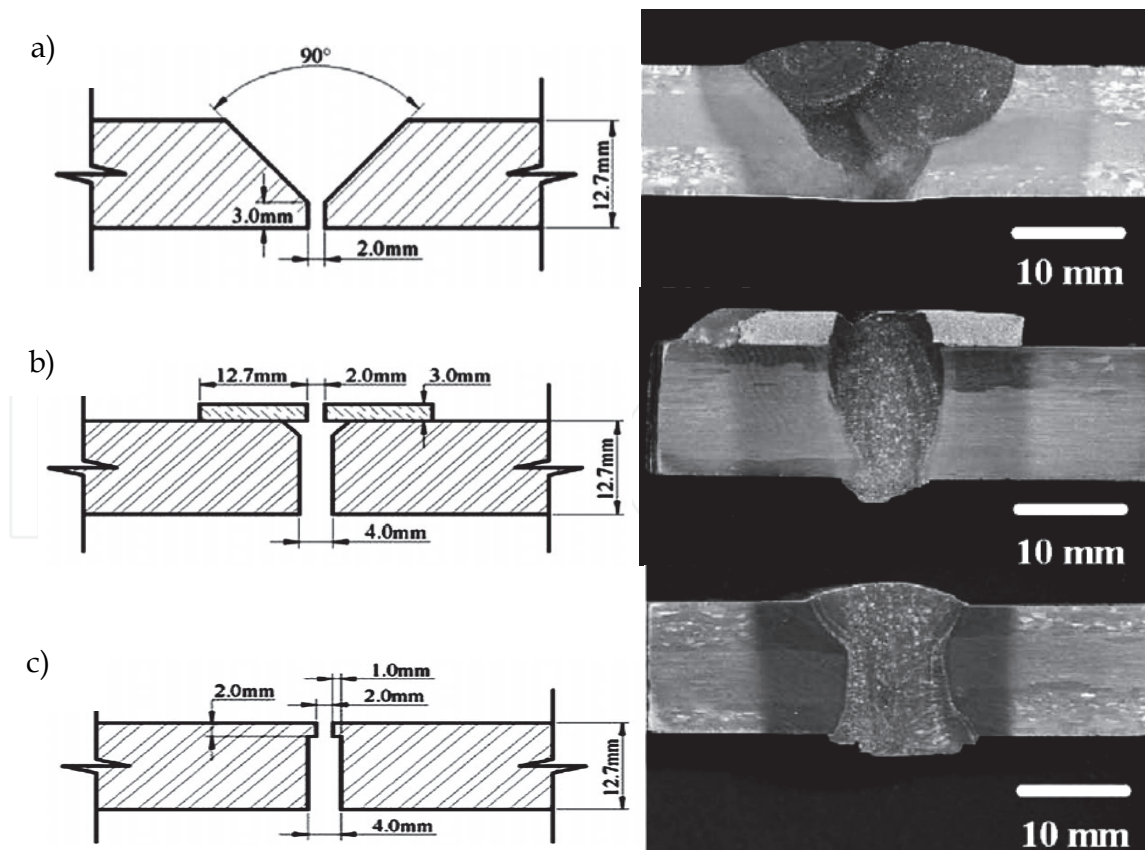


Fig. 3. Joint designs and typical geometry of the welds obtained; a) single V groove joint, b) IEA joint and c) MIEA joint.

The Fig. 3 shows different joint designs and dimensions as well as the typical geometries of the welds obtained by a) typical single V groove joint, b) IEA joint and c) MIEA joint. Whilst for the single V groove joint three or more welding passes are required to fill the groove, the IEA and MIEA joints only need one welding pass. The macrographs of the transverse weld profiles depict the geometries of the weld beads. Macroetching of the welds also revealed the HAZ. Roughly, it can be seen the larger thermal affection in the single V groove joint as compared to the IEA and MIEA welds.

3. Applications of the IEA welding process

In this section, an overview of the findings and benefits observed in different materials are provided. Between these materials are the MMCs, aluminium and its alloys and carbon steels.

3.1 Composites

The development of MMCs was a breakthrough in materials technology in the 80's. Acceptation and use of new materials rely on their readiness to be joined. Sorting out the challenges of incorporating ceramic reinforcements into molten metals and alloys was not enough for spreading the use of MMCs. A major problem was also encountered when trying to join this type of materials with conventional fusion welding processes. Exposure of the Al/SiC-type composite to temperature above the liquidus of the aluminium alloys, as typically experienced in welding, results in a severe lose of mechanical properties due to the formation of brittle and hygroscopic aluminium-carbon compounds, mainly aluminium carbide. In addition, fusion welding processes produce a weld pool that has poor fluidity and solidifies with large volumes of porosity in the weld, because of the realization of hydrogen from the melted aluminium powder, which is used to make many MMCs (Ahearn et al. 1982). A reduction in the porosity in welds deposited by gas tungsten arc welding (GTAW) was achieved by previous vacuum degassing for long periods of time before welding. Nevertheless, both Al_4C_3 and Al-Si eutectic were detected in degassed composites. A number of authors (Cola & Lundin, 1989; Devletian 1987; Fukumoto & Linert, 1993; J Ahearn, et al, 1982, Ellis, et al, 1995; Urena et al, 2000, Lundin et al, 1989, Lienert, et al, 1993) reported that Al_4C_3 is always formed in the weld metal in MMCs reinforced with SiC no matter which of the fusion welding processes is employed to weld the MMCs (laser, electron beam, TIG, MIG and so on), and the formation of this compound occurs according to Eq. (1).



This reaction is not reversible and the Al_4C_3 is formed as plates in the microstructure. The presence of the plates has two deleterious effects. First, the material becomes extremely brittle, and second, it becomes very prone to corrosion in presence of water, leading to the release of acetylene gas. In an extreme case, this has led to total corrosion of the weld within a few days. In response to the problematic issue of welding MMCs, the idea of the indirect electric arc was conceived (Garcia et al 2002) with the metal inert gas (MIG) welding process in order to overcome the difficulties of welding MMCs. The concept is based on the fact that experimental measurements indicate that the temperature of the droplets in the MIG welding process with spray transfer is between 2000 to 2327 °C for aluminium and its alloys according to (Lu & Kou, 1989, Kim et al, 1991). If a molten metal with a large overheating is

casted into a "mould" shaped by the parent materials to be welded, the sensible heat of the weld pool formed is sufficient to melt the side walls (the matrix in MMCs) whilst instantly filling the groove, yielding the welded joint upon freezing. The indirect application of the electric arc reduces the degradation of the ceramic but still the temperature of the molten metal is large to induce spontaneous and instantaneous wetting so that continuity is seen between weld metal and the matrix of the composites when the content of reinforcement is large (Garcia et al, 2002, 2003) and significant incorporation of particles into the weld metal occurs for composites with low fraction of reinforcement (Garcia et al, 2002, 2007).

The MIG welding process with IEA is a novel fusion welding method, which was developed to join MMCs with a reduced HAZ in the base metal. In the IEA welding method, the fusion of the base metal is not caused by direct contact with the electric arc, instead, the electric arc is established between the solid electrode and a plate of the same base metal, placed over the parent material. The resultant droplets, in the form of a spray, produce a molten pool on the plates and the liquid is fed instantaneously at high temperature into the groove formed by the base metal; Fig. 4 depicts the experimental set-up in a dissimilar join. Experimental measurement indicate that the droplets temperature in the MIG welding process with spray transfer is between 2000 to 2327 °C for aluminium and its alloys according to (Lu & Kou, 1989, Kim et al, 1991). As a result of its elevated temperature, the liquid metal melts the parent materials (the matrix in MMCs), yielding the welded joint upon freezing.

Profiles of MMCs welds using IEA are shown in Fig.4. Irrespective of the reinforcement content (high, medium or null), full penetration was attained in one welding pass and uniform weld profiles are obtained with little fusion of the base materials and a minimized heat input. The contour of the weld at the top depicts the configuration of the electric arc, which does not impinge on the surface of the parent plates; rather, it strikes inside the channel formed by them, as illustrated previously in Fig.1. Thus, during welding the electric arc is hidden and the typical flashing and sputtering of the normal MIG welding process is no longer observed when welding is carried out in any kind of material. It is well known that in order to weld 9, 10 mm thick MMCs and 12.5 mm thick aluminium plates, conventional MIG welding practice demands more than one welding pass with low travel speed, which leads to a large HAZ. It is worthy bearing in mind that most of the attempts to weld MMCs have been performed rather in thin sections or depositing bead on plate welds.

It has been reported during MMCs welding by different welding processes, that the high energy developed by the electric arc produces a wide HAZ accompanied by dissociation of the ceramic particles and the formation of hygroscopic compounds (Al_4C_3). This was confirmed by (Garcia et al, 2007) when welding an A359/SiC/20p commercial composite. Fig. 5a shows jagged SiC particles within the weld metal, this feature was not seen when the composite was welded with IEA. Fig 5b shows also the particles incorporated into the weld metal but they retain their initial angularity meaning that significant degradation (according to the resolution of the optical microscope) did not occur during welding with IEA. Tensile testing of the welded joints drew a tensile strength of 234 MPa for the IEA weld (one welding pass) as compared to 209 MPa for the weld with direct application of the electric arc (three welding passes). This behaviour is related to a larger incorporation of SiC particles into the weld metal and the reduced porosity for the IEA weld. The authors stated that the degradation of the SiC particles observed in the plain weld played a minor role during mechanical testing.

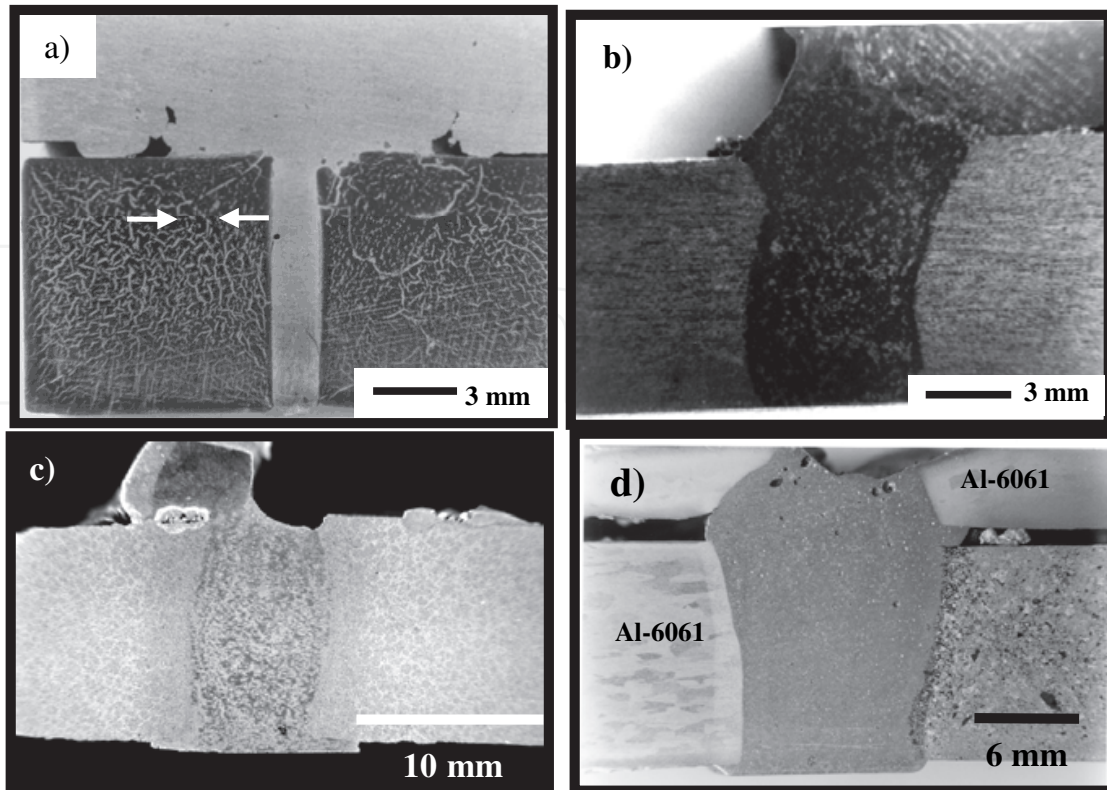


Fig. 4. Weld profiles obtained with the MIG-IEA technique in different MMCs.

a) Al-1010/TiC/50p (Garcia et al, 2003), b) Al-6061/Al₂O₃/20p (Garcia et al, 2002), c) A359/SiC/20p and d) dissimilar joint.

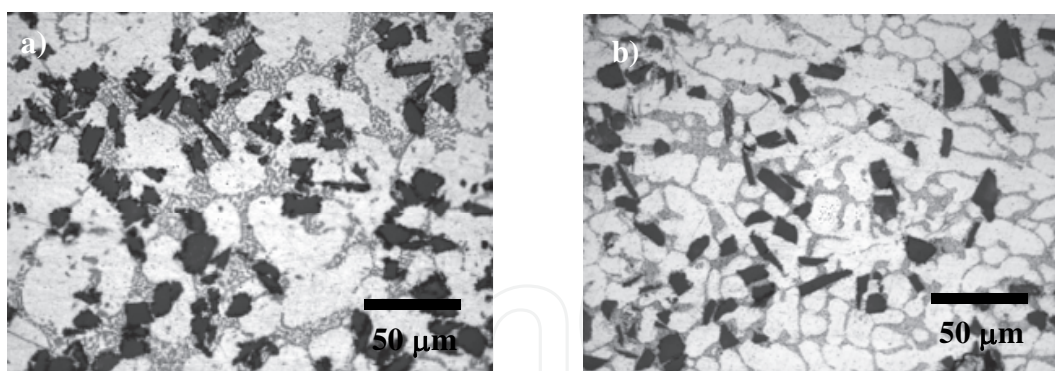


Fig. 5. Effect of the a) direct and b) indirect application of the electric arc on the SiC particles during welding an A359/SiC/20p commercial composite (Garcia et al, 2007).

3.2 Carbon steels

Pipelines of low carbon steel welded by electric arc have been used for many years and are widely used in the petroleum industry. However, frequent failures during operation over the years have prompted several studies of the design, construction, operation and maintenance of equipment and metallic structures used in this industry (Craig, 1997). Oil and gas from Mexico contain high concentrations of H₂S and CO₂, these constituents induce failures. In the oil industry, the welding processes commonly used for joining pipeline are electrical resistance (ERW) and submerged arc welding (SAW). With these processes, wide

HAZs are created and as a result, a high probability of cracking due to the heterogeneous weldment exists. Studies of weld bead failures have demonstrated that these occur mainly in the HAZ because of the variation in microstructure (grain growth), residual stresses and a higher susceptibility to embrittlement by hydrogen. These microstructures are produced by the thermal gradients experienced in the joint during welding. Therefore, it is very important to develop welding processes with a narrow HAZs, this is possible with the IEA process. The welding process has an important influence in the SSC susceptibility of materials. The different welding processes promote different changes in the microstructure of the welded zone; these changes affect the SCC resistance and the yield strength of the pipeline steel.

A comparative study of SSC resistance between IEA, SAW and MIG was carried out (Natividad et. al., 2007) through slow strain rate tests (SSRT), electrochemical tests and hydrogen permeation measurements. The base metal used was API grade X-65 pipeline steel. Cylindrical tensile specimens with a gauge length of 25 mm and gauge diameter of 2.50 mm were machined from the pipeline perpendicular to the rolling direction. The specimens were subjected to conventional slow strain rate tests in air (as an inert environment) and in the standard NACE solution (5% NaCl, 0.5% acetic acid, saturated with hydrogen sulphide (H₂S)) at a strain rate of 1x10⁻⁶ s⁻¹ at room temperature (25°C) and at 37°C and 50°C. All of the tests were performed at the open circuit potential (OCP). The loss in ductility was assessed in terms of the percentage reduction in cross-sectional area (% RA), as follows

$$\%RA = \frac{A_1 - A_f}{A_f} \times 100 \quad (2)$$

where A_i and A_f are the initial and final cross-sectional areas, respectively. The index of susceptibility to SSC (I_{SSC}) was calculated as follows

$$I_{SSC} = \frac{\%RA_{AIR} - \%RA_{NACE}}{\%RA_{AIR}} \quad (3)$$

where % RA_{AIR} and % RA_{NACE} are the percentage reduction in area values in air and in the H₂S-saturated NACE solution, respectively. An I_{SSC} value close to unity indicates high susceptibility towards SSC whereas a value close to zero indicates immunity. The fracture surfaces were then examined using scanning electron microscopy (SEM).

Fig. 6 shows the macro and microstructures of the weldments obtained by the three welding processes. This figure shows clearly the different zones: base metal (BM), weld bead (WB), HAZ and fusion zone (FZ). Full penetration and a narrow HAZ are observed in microstructure obtained by IEA process. The weld bead and HAZ is very different from that obtained by both SAW and MIG processes. In general, the microstructure obtained with the IEA welding process is more homogeneous than the obtained by SAW and MIG processes. The corrosion and the SSC susceptibility of the welds are affected by the differences in composition, microstructure, and electrochemical potentials among the different zones. A lower electrochemical potential of the weld bead is commonly related to composition, microstructure and distribution of inclusions (Dawson et. al., 1997). Similarly, in a study performed by Turnbull and Nimmo, about SCC susceptibility (Turnbull & Nimmo, 2005), a direct relation to OCPs with mechanical properties like microstructure or hardness of phases was reported.

The limit of hardness recommended for avoiding cracking in a sour environment is 22 Rc (248 Hv) (NACE/ISO, 2009). Although susceptibility to SSC generally increases with increasing hardness, some microstructures are more susceptible to cracking than others at the same hardness. Fig. 7 shows hardness measurements obtained from a transverse section of the weld for each welding process and it is observed that the values of hardness in the weld bead made by the SAW process are the lowest. For the MIG process, there is no significant difference between the HAZ and the WB hardness values. On the other hand, for the IEA process, the hardness value of the HAZ decreases by nearly 35 HV with respect to weld bead values. These values are within the recommended limits to avoid the fracture and cracking of the weld bead.

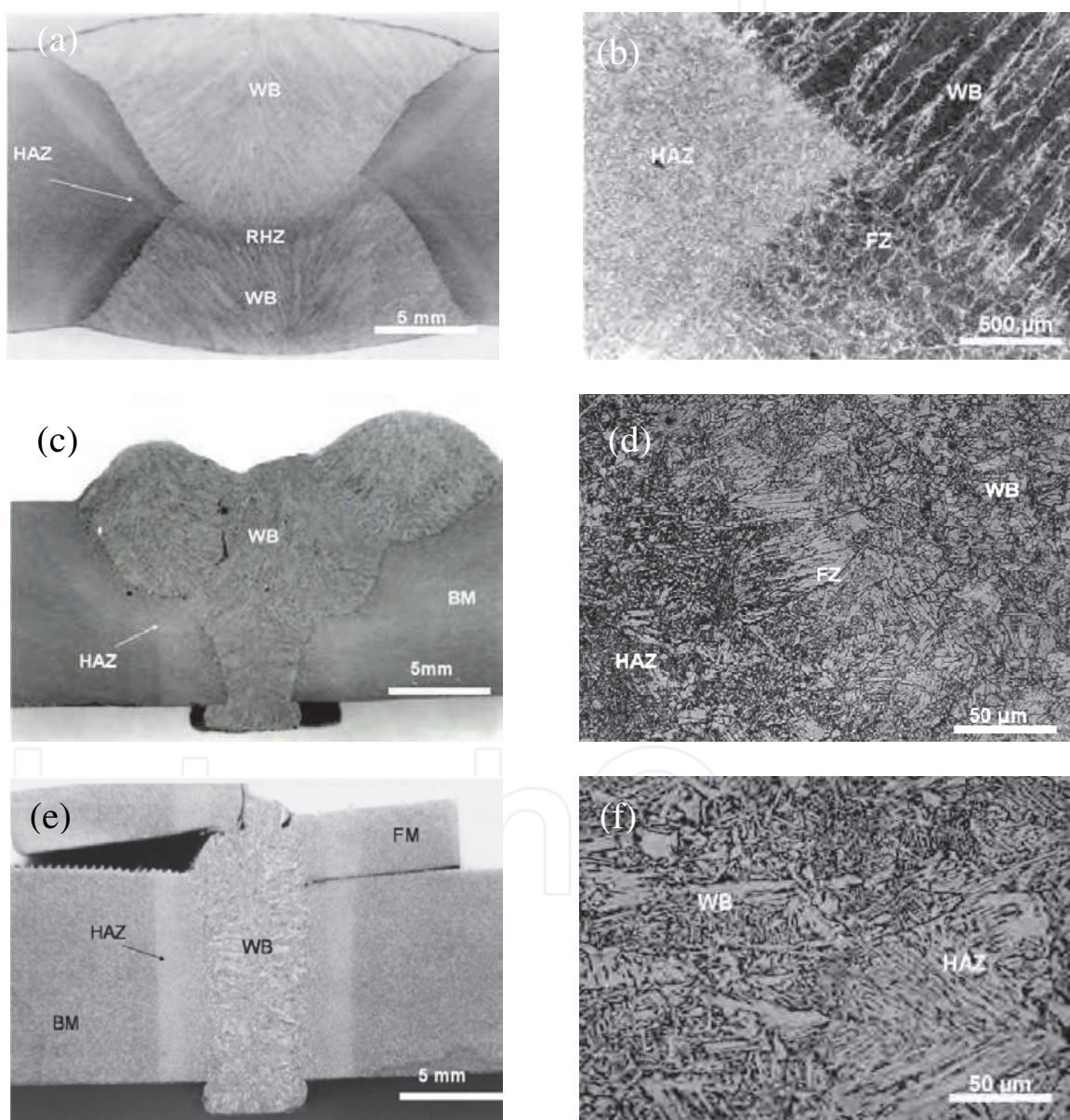


Fig. 6. Macro and microstructures of the weldments obtained by (a-b) SAW, (c-d) MIG and (e-f) IEA, (Natividad et al., 2007).

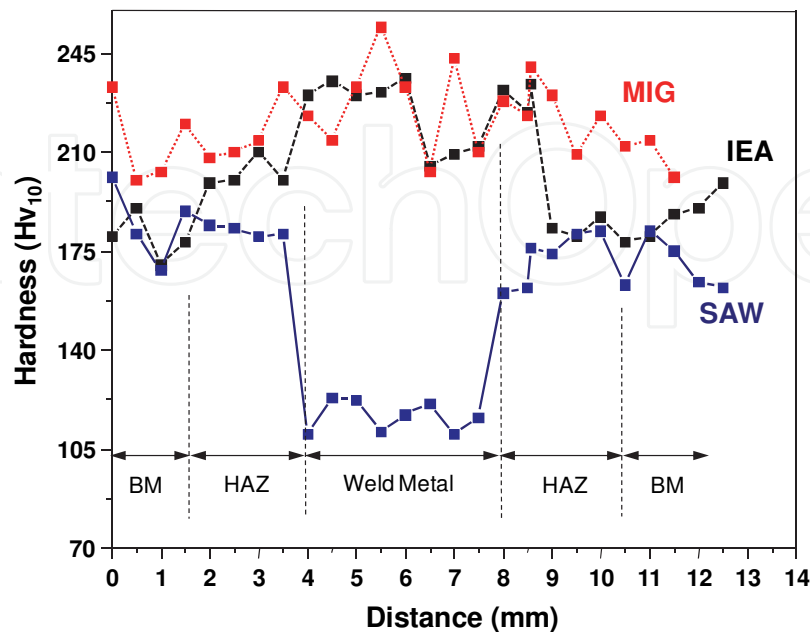


Fig. 7. Hardness values in weldments obtained by the different welding processes. (Natividad et al., 2007).

Fig. 8 shows the I_{SCC} measurements on the three weldments at the three bath temperatures. The welded joint obtained by SAW shows the highest I_{SCC} values, which was correlated with the hydrogen permeation results. Similarly, the I_{SCC} measurements in the IEA case indicate a lower concentration of both the trap sites in the metal and the susceptibility to hydrogen embrittlement, because here the most hydrogen flux passed to the anodic cell side. Although the high electrochemical activity generates a higher atomic hydrogen concentration, a smaller concentration of this atomic hydrogen was trapped in the bulk. In addition, the I_{SCC} results were affected by the change of welded microstructure, where the IEA presented a refined higher concentration of bainite compared with the grain coarse ferrite+pearlite microstructure obtained by the SAW process as reported before (Turnbull & Nimmo, 2005), and the consequent change in hardness due to the modified grain size during welding process (Omweg et al, 2003). Some evidence of the hydrogen diffusion effect into the welded joints is presented in the SCC fractographs illustrated in Fig. 9. The SAW weldments (Fig. 9b) show a more brittle fracture than the MIG and IEA weldments. The IEA weldment presented a less brittle fracture (Fig. 9a) and the I_{SCC} values show this behaviour. However, the three welded joints do not show a completely brittle behaviour, but in general, the fracture behaviour was closer to a quasi-cleavage fracture. The hydrogen diffusion was low in quantity and low in permanence time into the electrolyte generating hydrogen embrittlement, but there is evidence of the hydrogen damage to the weldments. Additionally in this work, the IEA material was the least susceptible to hydrogen embrittlement damage, of course, the SCC resistance was higher, and was related to the lowest OCP activity promoted by the change in microstructure of the weldment.

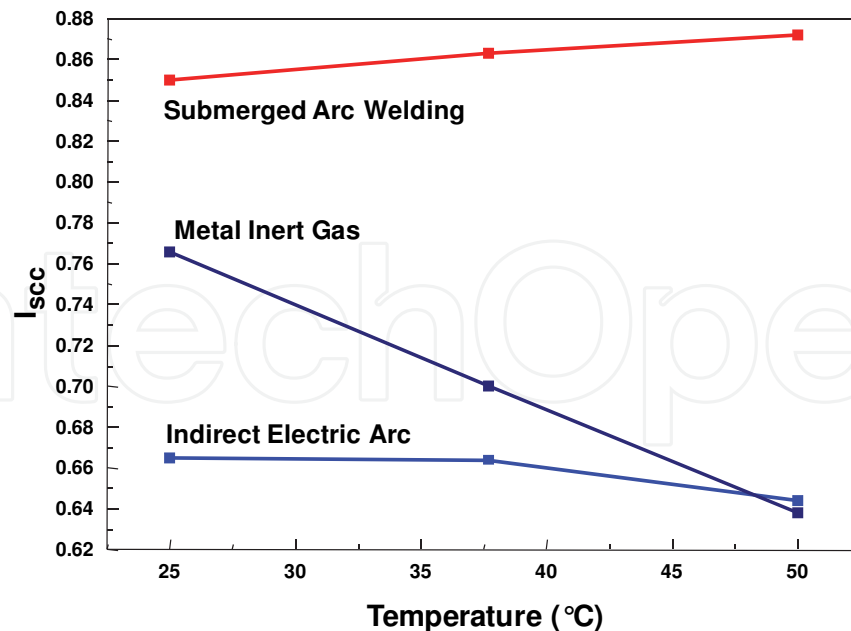


Fig. 8. Variation of I_{scc} as function of temperature on the weldments (Natividad et al., 2007).

With the features of the IEA process, a better SSC resistance at 25 °C was obtained in comparison to the SAW and MIG processes. For specimens obtained by the IEA process subjected to SSR tests, the failure occurred on the base metal and for specimens produced by SAW and MIG processes it occurred in the weld bead and HAZ respectively. At 37 °C and 50 °C, the SSC resistance of all processes show a similar behaviour (failed in the base metal). The higher atomic hydrogen permeation flux presented by the IEA process was promoted by the ferrite phase from the base metal, which is comparable to the fracture which occurred from SSRT.

A significant increase in the corrosion current (more positive OCP) was presented by the IEA material, and was attributed to the greatest galvanic cell formation between the welded and base metal, but this material shows superior resistance to the SCC susceptibility than that for the MIG and SAW processes. The hydrogen permeation results and the difference in microstructure presented by the IEA process corroborate this behaviour.

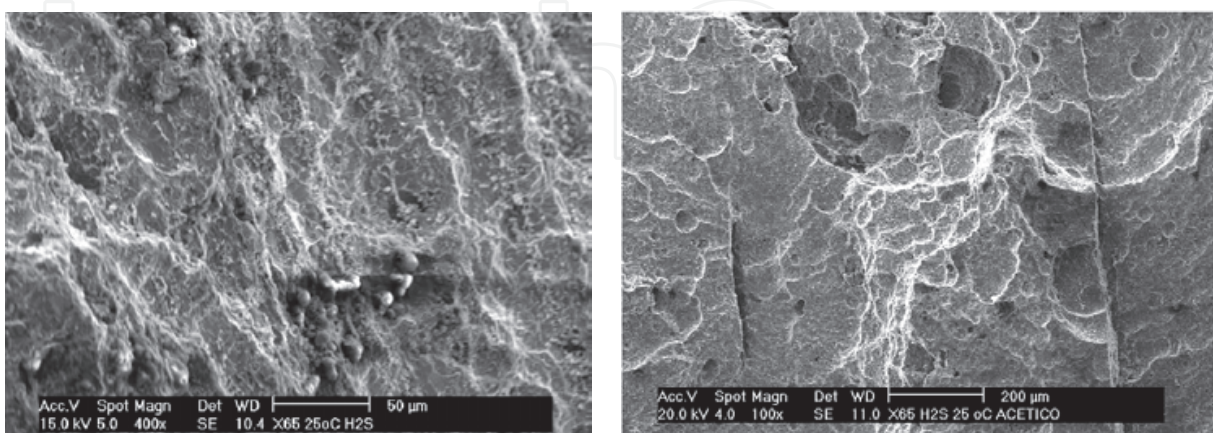


Fig. 9. SEM images of the SCC fractographies of (a) IEA weldment material and (b) SAW weldment material tested at 25 °C into the NACE solution saturated with H_2S , (Natividad et al., 2007).

3.3 Aluminium and Al-alloys

Aluminium and its alloys are important engineering materials with a vast number of applications as structural and functional components. The shiny and attractive appearance of these materials is due to the native oxide layer that always envelops the bulk of the material. The aluminium oxide layer is highly compact and this characteristic prevents further thickening of the oxide and permeation of aggressive media, making of Al and its alloys corrosion resistant materials in a number of environments. Besides, their lightness means a large strength/weight ratio for heat treatable Al-alloys (Davies, 1993 & Heinz et al, 1990). The high technological relevance of Al and its alloys demands quite often joining operations. The first barrier to overcome for successful joining is the native oxide layer which avoids coalescence between faying surfaces. In order to succeed fusion welding with the electric arc, direct current and reverse polarity are used to generate an ionic striking effect that dissolves the oxide and enables mixing between molten metals. Another aspect to take into consideration is the high solubility of hydrogen in aluminium melts. If care is not taken in preventing sources of hydrogen during welding, this effect may lead to welds with a large level of porosity in the weld metal. Besides, Al-alloys are prone to solidification and liquation cracking owing to their relatively high thermal expansion, large change in volume upon freezing as well as wide solidification temperature range (Gittos et al, 1981; Enjo & Kuroda, 1982; Kerr & Katoh, 1987; Miyazaki et al, 1990; Malin, 1995; Huang & Kou, 2004). All the above mentioned defects may have a profound impact on the mechanical performance of the welded joint and therefore they must be prevented. Furthermore, exposure of heat treatable Al-alloys to the welding thermal cycles gives rise to a soft zone in the HAZ caused by overaging where the mechanical strength may decrease up to 50% (Malin, 1995). Partial or almost full recovery of the mechanical properties can be achieved by post weld heat treating (solutioning, quenching and aging) but this procedure might be restricted in many instances and the welded joint must be on service in the as-welded condition. On this context, contributions aimed to improve the mechanical performance of aluminium alloys are desirable and valuable.

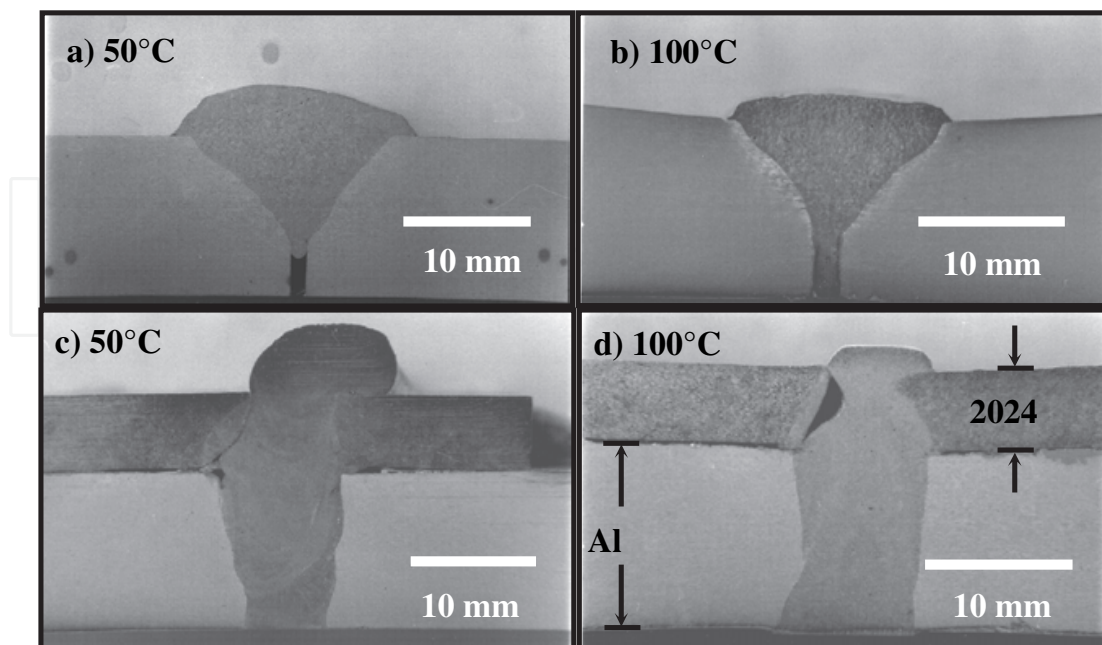


Fig. 10. Comparison of the weld profiles obtained with the direct (a-b) and indirect (c-d) application of the electric arc with preheating of the joint (Garcia et al, 2007).

The IEA technique developed by (Garcia et al, 2002) was applied to study the feasibility of welding Al and its alloys by using an ER4043 filler wire. Preliminary welding trials (Garcia et al, 2007), in plates of aluminium of commercial purity, revealed that the IEA technique has the capability of joining plates of 12.5 mm in thickness in a single welding pass with full penetration by preheating the plates to 50 or 100°C as shown in Fig. 10. Conversely, with the same preparation of the parent plates but without the feeding plates, welds with partial penetration are obtained as seen in Fig. 10. Needless to say, this problem shows why traditionally welding of thick sections is performed by a multi-pass procedure either with a single or double V preparation of the plates.

Microstructural characterization of the welds disclosed for the welds with direct application of the electric arc the typical epitaxial and columnar grain growth from the partially melted grains of the base metal whereas for the IEA welds, partially melted grains of the base metal were found trapped within the weld metal as shown in Fig. 11. The mechanism of this phenomenon was previously mentioned in section 2. Dragging and survival of partially melted grains modified the mode of solidification in the weld metal by blocking columnar growth. Thermal analysis of the IEA technique showed that heat losses by radiation and convection are reduced since the electric arc is established in a hidden fashion within the channel formed by the feeding plates. The authors stated that the low ionization potential of the aluminium vapour, 5.986 eV, plays also an important role in the IEA technique.

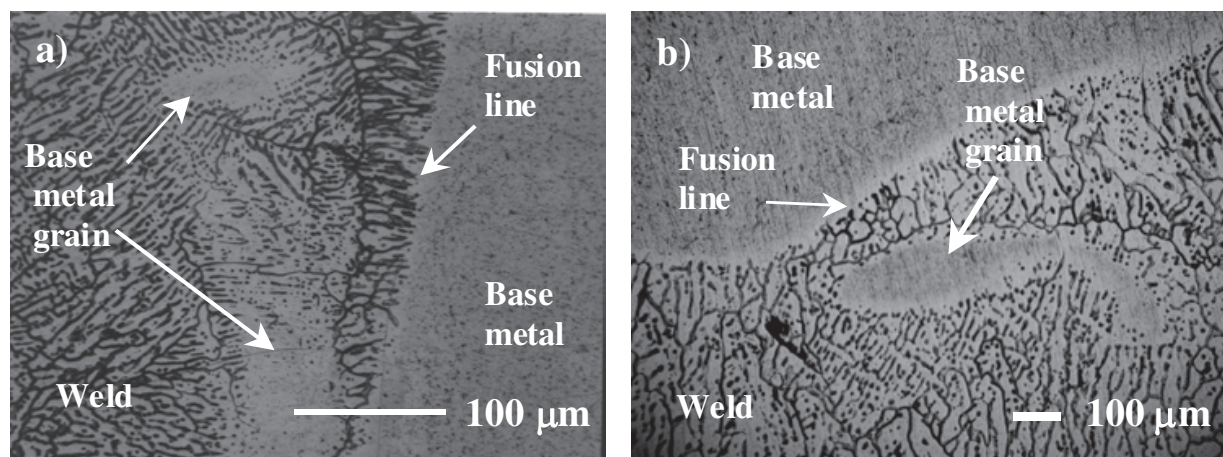


Fig. 11. Optical micrographs of the base metal/weld interface: (a) in the transversal and (b) longitudinal axes of a MIG-IEA weld (Garcia et al, 2007).

The preliminary findings suggested that if the number of welding passes are reduced, so it is the heat input. This advantage means also a reduction in the thermal affection of the base metal and therefore a minimization in the loss of strength in heat treatable aluminium alloys. To prove this, plates of an Al-6061-T6 were welded with the IEA technique and the results were compared with a single V joint (Ambriz et al, 2009). Table 1 shows the results of the mechanical properties under tension of the welded joints in the as-welded condition. At first sight, it is clear that the mechanical properties are lower than the base metal independently of the joint design employed. The worst mechanical properties were, however, exhibited by the single V-groove joint, which has approximately 37.4 and 61% mechanical efficiency with respect to base material and filler wire respectively. In comparison to the single V groove joint, the IEA joints exhibited a notable increase in the

mechanical efficiency with values ranging between 48 to 55%. Nevertheless, those efficiencies are still below the permissible limit of 57% for the 6061-T6 alloy according to the ASME Pressure Vessel Code, Section VIII. Irrespective of the joint design and preheating condition, the mechanical failure under tensile testing occurred in the base metal, at different distances from the fusion line, depending on joint design and preheating condition. The nearest failure from the fusion line occurred for the single V joint.

Joint type	Preheating temperature (°C)	Ultimate strength (MPa)	Yield strength (MPa)	Elongation (%)	Failure from fusion line (mm)	Efficiency from base metal (%)	Efficiency from filler metal (%)
ER-4043	--	190	164	--	--	--	--
6061-T6	--	328	300	14	--	--	--
DEA	25	116	57	17.6	3	35.36	61.05
IEA	50	148.9	71.6	14	11-13	45.39	78.36
IEA	100	172.1	76.8	14.8	13-15	52.46	90.57
IEA	150	168	86.7	15.2	13-16	51.21	88.42

Table 1. Mechanical properties of the weldments in the as-welded condition (Ambriz et al, 2009).

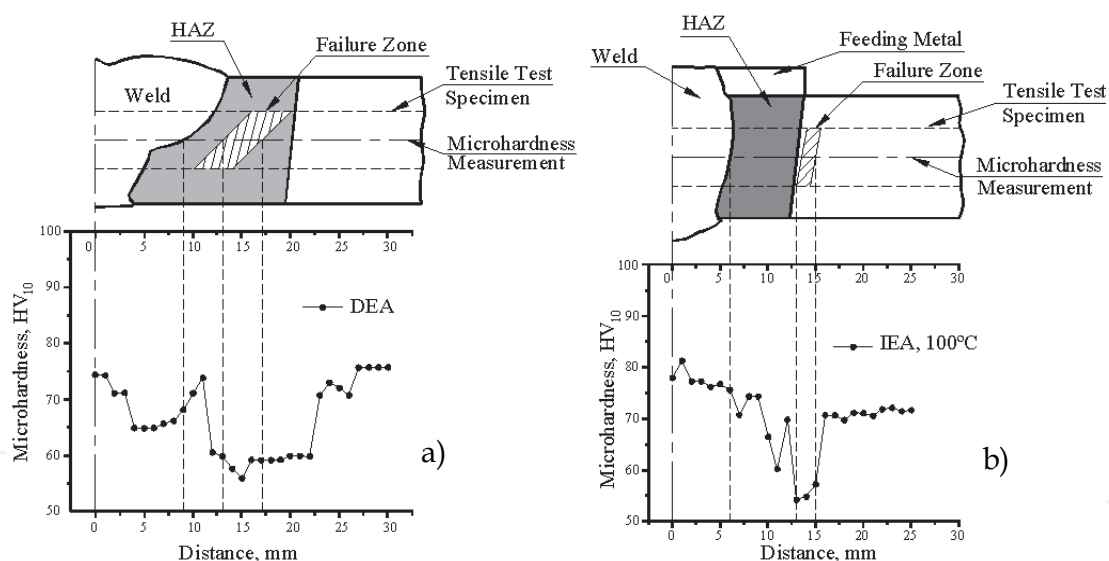


Fig. 12. Microhardness profiles for; a) the single V joint and b) the IEA joint preheated to 100°C (Ambriz et al, 2009).

Fig. 12 shows microhardness profiles along the cross sections of the welds, they corroborate the failure zone with the variation of mechanical properties, as a result of the thermal cycle of welding. The plots of these figures reveal, in each weld, a soft zone which matches well with the failure zone of the tensile specimens. This behavior, which nevertheless was expected, agrees with others (Gutierrez et al, 1996; Liu et al, 1991; Myhr et al, 2004; Shelwatkar, 2002; Kostivas & Lippold, 2000). Worth to point out is the fact that the depth, in terms of microhardness, and width of the soft zone is related to the joint design and preheating temperature. These features are obviously reflected on the tensile strength of the welds. Note that although the IEA and single V groove are similarly "soft", the later fails

with a lower stress due to the relaxation of the dislocations as a result of repeated exposure to heat. Another important aspect revealed by the microhardness profiles is the increase in hardness within the weld metal for the IEA joint as compared to the single V groove joint. This trend is related to the dilution rates for each joint, the larger the dilution the largest incorporation of alloying elements into the weld metal, and to the solidification mode inherent to every joint design. Whilst the single V groove joints exhibits the typical epitaxial and competitive-columnar grain growth, the IEA joints solidified with a grain refined microstructure.

4. Modified indirect electric arc (MIEA)

The main disadvantage of the IEA technique is that it leaves the residual feeding plates on top of the welded joint. This would be unacceptable in most of the applications. Thus, an additional step in the process demands removing these strips from the weld. To overcome this inconvenient, a modification of the design of the IEA joint was proposed and tested in heat treatable aluminum alloys. The use of the strips of feeding material on top of the work pieces was omitted and in the upper part of the work pieces a lash was machined, simulating the original feeding plates. This evolution was named MIEA (Ambriz et al., 2006, Ambriz et al. 2008). The MIEA provided several advantages with respect to the traditional arc fusion welding process, for instance:

- i. The high thermal efficiency that allows welding plates by using a single welding pass. As a result, the thermal effect is reduced and the mechanical properties of the HAZ are improved as compared to a multi-pass welding procedure,
- ii. The dilution percent of the weld pool is higher; which tends to improve the hardening effect after performing a post weld heat treatment (PWHT) (Ambriz et al., 2008),
- iii. The solidification mode promotes an heterogeneous nucleation and jointly diminishes the micro-porosity formation,
- iv. The geometry of the welding profile improves the fatigue performance of the welded joint (Ambriz et al., 2010a).

MIEA welding technique employs the same equipment that is required to weld by GMAW. General dimensions and the schematic representation of the MIEA joint along with the weld bead geometry obtained were shown in Fig. 3c. The dissipation of heat in this case is quite similar to the IEA joint so that large thermal efficiency is also obtained.

4.1 Microstructure in aluminum alloys welds

In a fusion welding process, the heat input produces a fusion-solidification phenomenon, which is different to that obtained in the solidification of an ingot. (i) In an ingot, solidification begins with heterogeneous nucleation at the chill zone meanwhile in a weld pool the liquid metal partially wets the grains of the parent metal and epitaxial growth takes place from the partially melted grains of the parent metal (Davies et al., 1975). (ii) The rate of solidification in a weld pool, which depends on the traveling speed as well as the welding process, is by far faster than in an ingot. (iii) The macroscopic profile of the solid/liquid interface in welds progressively changes as a function of the traveling speed of the heat source whereas it exclusively depends on the time for an ingot. (iv) The movement of the liquid metal in a weld pool is greater than in an ingot due to the Lorentz forces which create turbulence within the molten metal (Grong, 1997). Fig. 13 shows longitudinal views, which depict the direction of solidification of the welds, for a multi-pass welding and MIEA with

preheating conditions at 50°C. The arrows indicate the displacing direction of the electric arc.

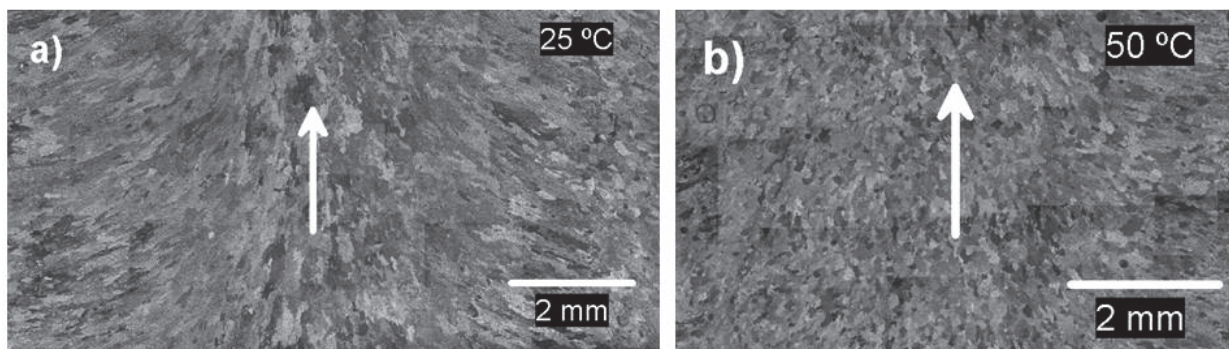


Fig. 13. Longitudinal top view of the weld metal grain structure at the mid plane for: a) single V groove, b) MIEA preheated at (50°C) (Ambriz, et al, 2010).

The longitudinal macrostructure for the MIEA joint, Fig. 13b, exhibit significant differences with respect to the multi-passes single V groove joint. Irrespective of the preheating condition, the local crystalline growth maintains an angle nearly constant in relation to the moving heat source. The virtual non existence of changes in growth direction means that the local and nominal rates of crystalline growth tend to be equal. This phenomenon yields a significantly different grain structure in the weld metal for the MIEA joint as compared to the structure observed for the single V groove joint. It leads, in fact, to a grain refining effect which is obviously affected by the initial preheating temperature of the joint.

The MIEA joint exhibits signs of heterogeneous nucleation which promotes grain refining. The levels of porosity in the MIEA joints decrease with preheating temperature and are comparatively lower than that obtained in the single V groove joint. Epitaxial solidification is also observed at the fusion line of the MIEA welds, however, competitive columnar growth was restricted instead grain structures alike those observed in the centre of the weld metal were present. The characteristics of solidification observed for the MIEA welds are the result of heterogeneous nucleation which is based on the principle of the formation of a critical radii needed to achieve the energy of formation from potential sites for nucleation such as inclusions, substrates or inoculants (Ti or Zr) (Rao et al., 2008; Ram et al., 2000; Lin et al., 2003). For the MIEA welds, these sites are principally the sidewalls of the joint in conjunction with the content of Ti in the filler and base metal since the significant dilution of base metal favors incorporation of Ti into the weld pool.

4.2 Mechanical properties in aluminum alloys welds

4.2.1 Microhardness

In order to determine the effect of the welding process in aluminum alloys, a common practice is to perform a microhardness profile in a perpendicular direction to the weld bead, as is showed in Fig. 14. Microhardness measurements give a general idea of the microstructural transformations and the variation of the local mechanical properties (Ambriz et al. 2011) produced after a welding process in aluminum alloys.

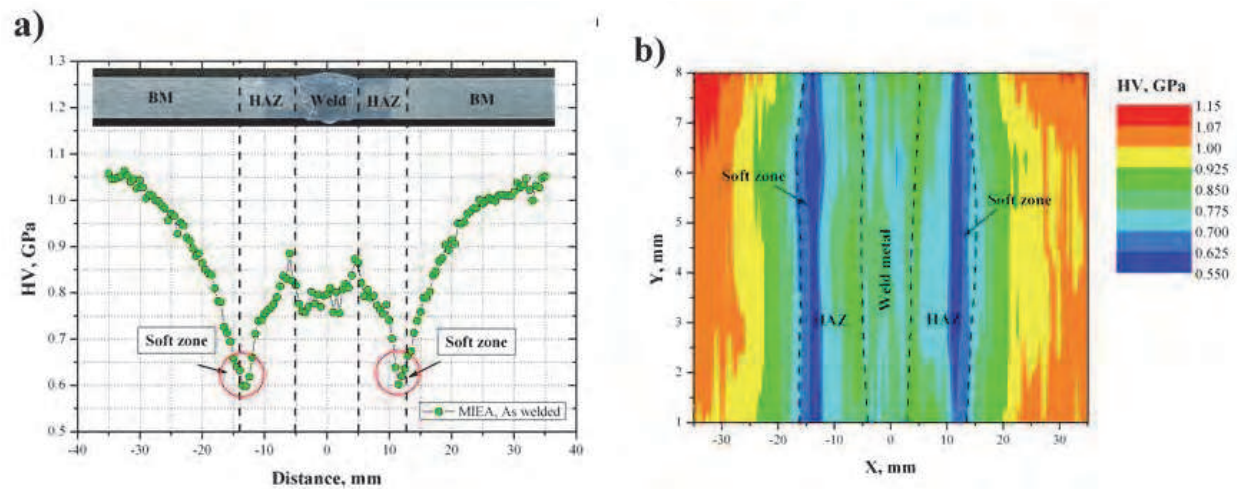


Fig. 14. a) Microhardness profile and b) microhardness map in 6061-T6 aluminum alloy welded by MIEA. Note that $1\text{HV}=9.8\times 10^{-3}\text{ GPa}$ (Ambriz, et al, 2011).

Fig. 14a presents the Vickers hardness number profile in 6061-T6 aluminum alloy welds obtained by MIEA. A significant difference between the hardness number of the weld material and HAZ with respect to the base material is observed. Also, at the limit between the HAZ and the base metal, it is noted the presence of a soft zone which is formed nearly symmetrically in both sides of the welded joints. It should be noted that the hardness obtained in this zone represents roughly 57 % of the hardness number of the base material. This seems to indicate that the tensile mechanical properties after welding process will be greatly different. Fig.14b visualizes the location of the soft zone highlighted by the Vickers hardness profile represented in Fig. 14a, by means of a hardness mapping. In this figure, the hardness values for each zone of the welded joint are well-defined. It is clear that in the soft zone (HAZ) the hardness number range is between 0.55 to 0.7 GPa. This soft zone results from the thermodynamic instability of the β'' needle-shaped precipitates (hard and fine precipitates) promoted by the high temperatures reached during a fusion welding process (Myhr et al., 2004). Indeed the temperatures reached during the welding process are favorable to transform the β' phase, rod-shaped, according to the transformation diagram for the 6061 alloy.

4.2.2 Tensile properties

The individual mechanical behaviour of the base metal, weld metal, HAZ and welded samples in as welded condition for 6061-T6 aluminum welds by MIEA is shown in Fig. 15 as stress as function of strain graph. From Fig. 15, it can be observed that the experimental results for the base metal are in agreement with nominal values found in the literature for 6061-T6 alloy (American Society for Metals Fatigue and Fracture, 1996). The tensile properties of the sample obtained from the HAZ presents a 41% and a 19 % reduction of the ultimate strength with respect to the base metal and weld metal respectively. The loss of mechanical strength commonly referred to as over-aging, when welding a 6061-T6 alloy is a fairly well understood phenomenon and it is explained in terms of the precipitation sequence (Dutta & Allen, 1991). During welding, however, the base metal adjacent to the fusion line is subjected to a gradient of temperature imposed by the welding thermal cycle. At certain distance from the fusion line, the cooling curve crosses the interval of temperatures between 383 to 250 °C in which the β' phase, rod-shaped, is stable. It is thus

the transformation of β'' into β' the responsible of the decrease in hardening of the α matrix due to the incoherence of the β' phase caused by the thermodynamic instability of β'' in a welding process. It is worthy to mention that the MIEA further increased the mechanical strength of this alloy as compared to the IEA joint (Ambriz et al, 2009).

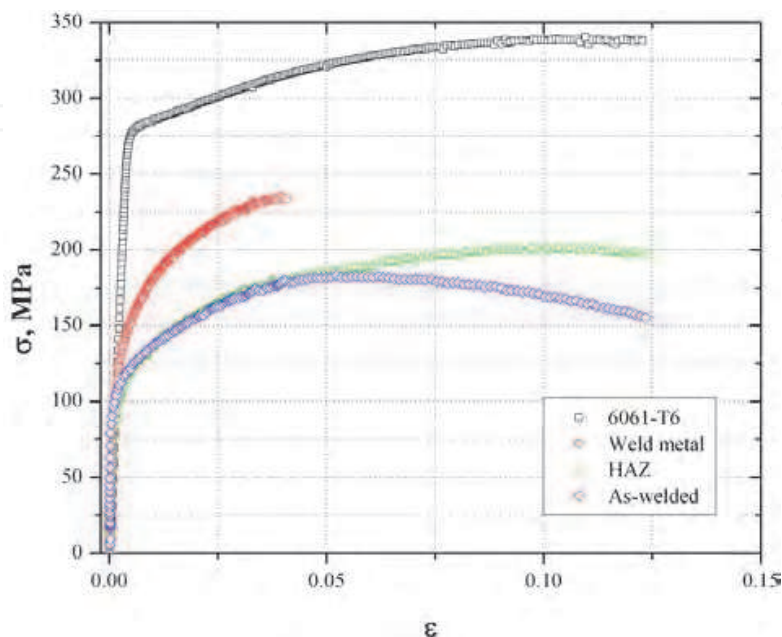


Fig. 15. True stress-strain curves for 6061-T6 plates, weld metal, HAZ and as welded (Ambriz et al, 2010).

4.2.3 Fatigue crack growth (FCG)

Fatigue behavior of aluminum alloys welded by conventional process and MIEA has been investigated (Ambriz et al. 2010b; Branza et al., 2009; Seto et al., 2004). Fig. 16a presents the crack length as a function of number of cycles for base metal, weld metal and HAZ in 6061-T6 welds by MIEA, for ΔP equal to 2.5 and 3.0 kN. In general, the $a-N$ curves showed in Fig. 16a reveal a notable difference in terms of crack length for each material as a function of the number of cycles, nevertheless the small change in ΔP (Ambriz et al., 2010b). Experimental results for a , were plotted in da/dN versus ΔK graphs according to Paris law:

$$\frac{da}{dN} = C(\Delta K)^n \quad (4)$$

where C and n are constants obtained directly from the fitting curve. Fig. 16b-d, presents the FCG data obtained for the base metal, weld metal and HAZ in MIEA, as well as the comparison with Friction Stir Welding (FSW) data found in the literature (Moreira et al., 2008). Fig. 16b, shows the FCG for base metal in both directions. This graph shows that the microstructure aspect (anisotropy) does not have an important influence in terms of FCG as could be expected, taking into consideration that yield strength in the base metal parallel to rolling direction is higher than transverse direction. However this is not the case for the weld metal and HAZ (Figs. 16c-d), in which the crack tend to propagate faster than base metal. Under this scenario, the FCG behavior for base metal (L-T) was taken as a basis to perform a comparative table between the weld metal and HAZ of MIEA and FSW. Table 2,

presents the crack growth rate, da/dN and the stress intensity factor ΔK , for base metal, weld metal and HAZ corresponding to a critical crack length in MIEA welds. For comparison effects, values for da/dN in MIEA were taken to compute the ΔK in FSW.

The results presented in Table 2 indicate that, there is an important difference in ΔK for weld metal and HAZ, independently of the welding process. In this way, it should note that ΔK for weld metal in MIEA represents only 57% of the base metal, unlike the ΔK for weld metal in FSW, which reach a 79% with respect to base metal. This means that FCG rate are higher in MIEA weld metal than FSW, as can be seen in Fig. 16c. This behavior is totally related to the joining processes; it means that MIEA is a welding technique based on a fusion welding process that employs a high silicon content filler metal, which produces a self grain refining, but a brittle microstructure in the weld metal (Ambriz et al., 2010b). On the other hand, FSW is a solid-state joining process that does not use a filler metal (Nandan et al., 2008). Thus, chemical composition in weld metal is similar to the base metal and microstructural characteristics related to dynamic recrystallization tends to be better than MIEA. In contrast, Fig. 16d shows that FCG rate in MIEA and FSW is similar in the HAZ. The stress intensity factor relation was 64% with respect to base metal. It is noted that thermal effect produced by the microstructural transformation of very fine precipitates needle shape β'' , to coarse bar shape β' precipitates, has a profound impact in the HAZ crack growth rate. It confirms that, independently of the welding process (MIEA and FSW), the crack growth conditions are directly influenced by the temperature within the HAZ, which is normally above of the aging temperature of the alloy, causing a hardening lost and important decrease in mechanical properties.

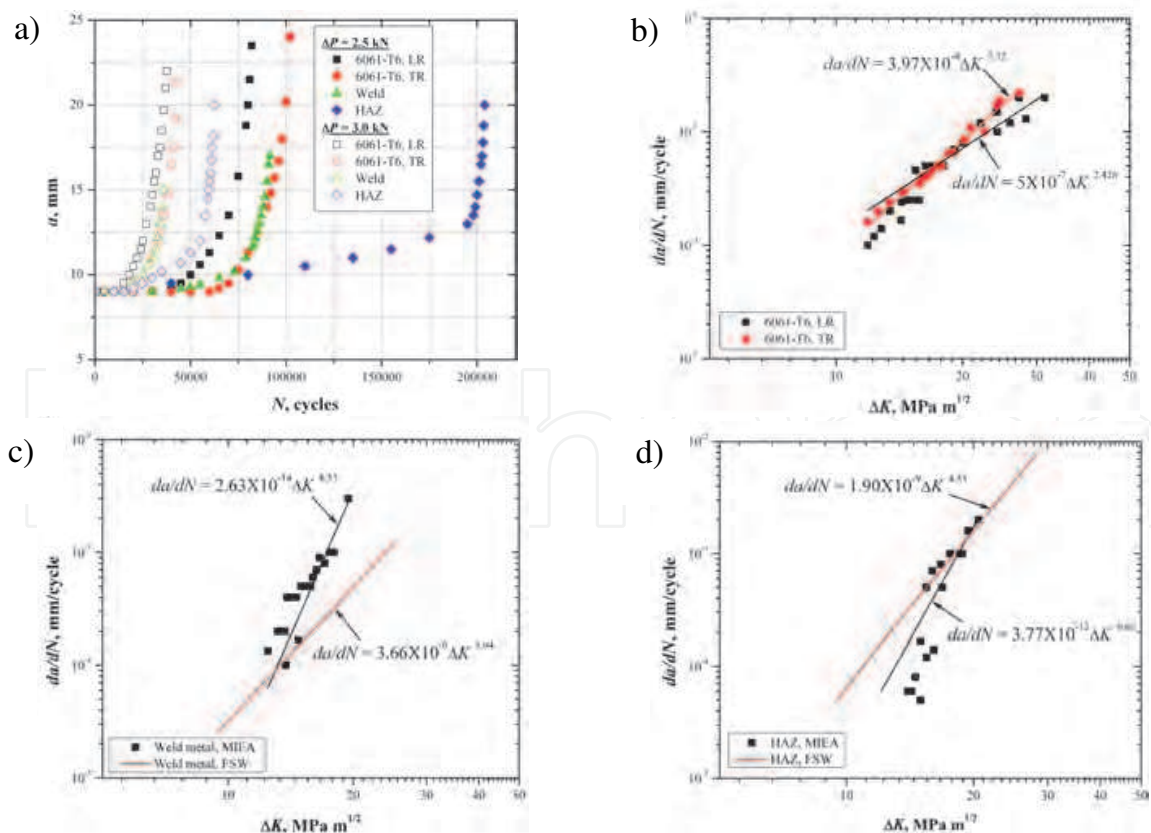


Fig. 16. a) crack length as function of number cycles, load ratio $R=0.1$, b-d) Fatigue crack growth rate as function of stress intensity factor range (Ambriz et al, 2010).

	Base metal	MIEA		FSW	
		Weld metal	HAZ	Weld metal	HAZ
da / dN (mm/cycle)	1.981×10^{-3}	1.0×10^{-3}	1.413×10^{-3}	1.0×10^{-3}	1.413×10^{-3}
ΔK (MPa m ^{1/2})	30.41	17.27	19.46	23.98	19.51
$(da/dN)_i / (da/dN)_{BM}$	1.0	0.50	0.71	0.50	0.71
$(\Delta K)_i / (\Delta K)_{BM}$	1.0	0.57	0.64	0.79	0.64

Table 2. Comparison between MIEA and FSW based on a critical crack length. BM = Base metal, *i* corresponds to weld metal or HAZ for MIEA or FSW (Ambriz et al, 2010).

5. Conclusions

The IEA technique and its evolution into the MIEA have emerged as an attractive alternative to weld a number of materials with peculiar microstructural characteristics that have a positive impact in the mechanical and stress corrosion cracking (SCC) behaviors. Between these material are aluminum metal matrix composites (MMCs) reinforced with TiC, SiC and Al₂O₃ particles and monolithic materials such as carbon steels (API X-60 and X-65), aluminum and its alloys, such as 6061, 2014 and 359.

With the IEA welding process, a columnar microstructure with a fine grain, more homogeneous structure and a small HAZ is obtained. In this process, the heat transfer developed does not affect the base metal as much as the direct electric arc process does, but the heat input is enough to partially melt the base metal yielding a weld profile with a high depth to-width ratio. In addition to the macroscopic features obtained, the use of this technique might lead to obtaining a fine microstructure in the weld for metallic materials and improved mechanical properties. The evolution into the MIEA has marked a significant progress regarding mechanical behavior as a result of the reduced thermal affection in heat treatable aluminum alloys.

6. References

- Ahearn, J.; Cook, C. & Fishman, S. (1982). Fusion welding of SiC-reinforced Al composites. *Metal construction*, Vol. 14, Issue 4 (April 1982), pp. 192-197, ISSN 03077896
- Ambriz, R.; Barrera, G. & García, R. (2006). Aluminum 6061-T6 welding by means of the modified indirect electric arc process. *Soldagem and Inspecao*, Vol. 11, Issue 1, pp. 10-17
- Ambriz, R.; Barrera, G.; García, R. & López V.H. (2008). Microstructure and heat treatment response of 2014-T6 GMAW welds obtained with a novel modified indirect electric arc joint. *Soldagem and Inspecao*, Vol. 13, Issue 3, (Jul-sep 2008), pp. 255-263, ISSN 0104-9224
- Ambriz, R.; Chicot, D.; Benseddiq, N.; Mesmacque, G. & de la Torre, S. (2011). Local mechanical properties of the 6061-T6 aluminium weld using micro-traction and instrumented indentation. *European Journal of Mechanics A/Solids*, Vol. 30, Issue 3, (May-Jun 2011), pp. 307-315, ISSN 0997-7538
- Ambriz, R.; Mesmacque, G.; Ruiz, A.; Amrouche, A. & López, V.H. (2010). Effect of the welding profile generated by the modified indirect electric arc technique on the

- fatigue behavior of 6061-T6 aluminum alloy. *Materials Science and Engineering A*, Vol. 527, Issue 7-8, (Mar 2010), pp. 2057-2064, ISSN 0921-5093
- Ambriz, R.; Mesmacque, G.; Ruiz, A.; Amrouche, A.; López, V.H. & Benseddiq, N. (2010). Fatigue crack growth under a constant amplitude loading of Al-6061-T6 welds obtained by modified indirect electric arc technique. *Science and Technology of Welding and Joining*, Vol. 15, Issue 6, (Aug 2010), pp. 514-521, ISSN 1362-1718
- Ambriz, R.R.; Barrera, G.; Garcia, R.; López, V.H. (2009). A comparative study of the mechanical properties of 6061-T6 GMA welds obtained by the indirect electric arc (IEA) and the modified indirect electric arc (MIEA). *Materials and Design*, Vol. 30, pp. 2446-2453. ISSN 0261-3069
- Branza, T.; Deschaux-Beaume, F.; Velay, V. & Lours, P. (2009). A microstructural and low-cycle fatigue investigation of weld-repaired heat-resistant cast steels. *Journal of Materials Processing Technology*, Vol. 209, Issue. 2, (Jan 2009), pp. 944-953, ISSN 0924-0136
- Cicala, E.; Duffet, G.; Andrzejewski, H.; Grevey, D. (2005). Hot cracking in Al-Mg-Si alloy laser welding - Operating parameters and their effects. *Materials Science and Engineering A*, Vol. A395, pp. 1-9, ISSN 0921-5093
- Cola, M.; Lienert, T.; Gouland, J. & Hurley, J. (1989). Laser welding of a SiC particulate reinforced aluminum metal matrix composite, *Proceedings of ASME 1 1989, International Conference on Recent trends in welding science and technology*, pp. 1297-303, Gatlinburg, Tennessee, USA, May 14-18, 1989, ISBN 0-87170-401-3
- Craig, B.D. (1998). Calculating the lowest failure pressure for electric resistance welded pipe. *Welding Journal*, Volume 77, Issue 1, (January 1998), pp. 61-63, ISSN 0043-2296
- Davies, G. & Garland J. (1975). Solidification structures and properties of fusion welds. *International Metals Review*, Vol. 20, (Jun 1975), pp. 83-106
- Davis, J. (1993). *Aluminium and aluminium alloys: ASM Specialty Handbook*, ASM International, New York, USA, ISBN 087170496X
- Dawson, J.; Palmer, J.; Moreland, P. & Dicken G. (1999). Weld corrosion-chemical, electrochemical and hydrodynamic issues, inconsistencies and model, *Proceeding of Advances in Corrosion Control and Materials in Oil and Gas Production EFC 26*, pp. 155-169, ISBN 1-86125-092-4, Trondheim, Norway, Sept 22-25, 1997
- Devletian, J. (1987). SiC/Al Metal matrix composite welding by a capacitor discharge process. *Welding Journal*, Vol. 66, Issue 6, (Jun 1987), pp. 33-39, ISSN 0043-2296
- Domey, J.; Aidun, D.; Ahmadi, G.; Regel L. & Wilcox W. (1995). Numerical - Simulation of the effect of gravity on weld pool shape. *Welding Journal*, Volume 74, Issue 8, (August 1995), pp. S263-S268, ISSN 0043-2296
- Dutta, I. & Allen, S. (1991). A calorimetric study of precipitation in commercial Al alloys. *Journal of Materials Science Letters*, Vol. 10, Issue 6, (Mar 1991), pp. 323-326, ISSN 0261-8028
- Enjo, T.; Kuroda, T. (1982). Microstructure in weld heat affected zone of Al-Mg-Si alloy. *Transactions of JWRI*, Vol.11, No.1, pp. 61-66, ISSN 0387-4508
- Fukumoto, S; Hirose, A. & Kobayashi, K. (1993). Application of laser beam welding to joining of continuous fiber reinforced composite to metal. *Materials science and technology*, Vol.9, Issue 3, (March 1993), pp. 264-271, ISSN 0267-0836

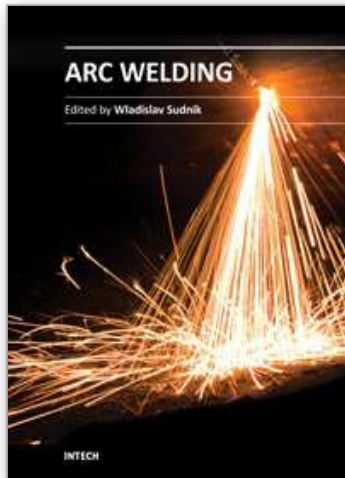
- García, R.; Lopez, V. H.; Bedolla, E.; Manzano, A. (2007). Welding of aluminium by the MIG process with indirect electric arc (MIG-IEA), *Journal of Materials Science*, Vol.42, pp. 7956-7963, (Jun 2007), ISSN 0022-2461
- García, R.; López, V.H.; Bedolla E. & Manzano A. (2002). MIG welding process with indirect electric arc. *Journal of Materials Science Letters*, Vol. 21, (2002), pp. 1965-1967, ISSN 0261-8028
- García, R.; López, V.H.; Bedolla E. & Manzano A. (2003). A comparative study of the MIG welding of Al/TiC composites using direct and indirect electric arc processes. *Journal of Materials Science*, Vol. 38, (2003), pp. 2771- 2779, ISSN 0022-2461
- García, R.; Manzano, A.; López, V.H. & Bedolla, E. (2002). Comparative welding study of metal matrix composites with the MIG welding process, using direct and indirect electric arc. *Metallurgical and Materials transactions B*, Vol. 33B, (December 2002), pp. 932 a 937, ISSN 1073-5615
- García, R.; López, V.H.; Kennedy, A. & Arias, G. (2007). Welding of Al-359/20%SiC_P metal matrix composites by the novel MIG process with indirect electric arc (IEA). *Journal of Materials Science*, Vol. 42, pp. 7794-7800, ISBN 0022-2461
- Gittos, N.; & Scott M. (1981). Heat-affected zone cracking of Al-Mg-Si alloys. *Welding Journal*, Vol.49, No.2, pp. 96-s-103-s, ISSN 0043-2296
- Grong, O. (1997). *Metallurgical Modeling of Welding*, (Second Edition), Maney Materials Science, ISBN 1861250363, London.
- Guitierrez, L.; Neye, G. & Zschech, E. (1996). Microstructure, hardness profile and tensile strength in welds of AA6013 T6 extrusions. *Welding Journal*, Vol.75, No.4, pp. 116s-121s, ISSN 0043-2296
- Heinz, A.; Haszler, A.; Keidel, C.; Moldenhauer, S.; Benedictus, R. & Miller, W. (2000). Recent development in aluminium alloys for aerospace applications. *Materials Science and Engineering A*, Vol. A280, No.1, pp. 102-107, ISSN 0921-5093
- Huang, C. & Kou, S. (2004). Liquation cracking in full-penetration Al-Mg-Si welds. *Welding Journal*. Vol. 83, No. 4, pp. 111s-122s, ISSN 0043-2296
- Kerr, H. & Katoh, M. (1987). Investigation of heat-affected zone cracking of GMA welds of Al-Mg-Si alloys using the varestreint test. *Welding Journal*, Vol.66, No. 9, pp. 251s-259s, ISSN 0043-2296
- Kluken, A. & Bjorneklett, B. (1997). A study of mechanical properties for aluminum GMA weldments. *Welding Journal*, Vol. 76, No.2, pp. 39-44, ISSN 0043-2296
- Lienert, T.; Brandon, E. & Lippold, J. (1993). Laser and Electron beam welding of a SiC_P reinforced aluminum A-356 metal matrix composite, *Scripta metallurgical et materialia*, Vol. 28, Issue 11 (Jun 1993), pp. 1341-1346, ISSN 0956-716X
- Lin, D.; Wang, G. & Srivatsan T. (2003). A mechanism for the formation of equiaxed grains in welds of aluminum-lithium alloy 2090. *Materials Science and Engineering A*, Vol. 351, Issue 1-2, (Jun 2003), pp. 304-309, ISSN 0921-5093
- Liu, G.; Murr, L.; Niou, C.; McClure, J. & Vega, F. (1997). Microstructural aspects friction-stir welding of 6061-T6 aluminum. *Scripta Materialia*, Vol.37, No.3, pp. 355-361, ISSN 1359-6462
- Liu, W. J.; Tian, X. & Zhang, X. (1996). Preventing weld hot cracking by synchronous rolling during weld. *Welding Journal*, Vol.75, No.9, pp. 297-s-304-s, ISSN 0043-2296

- Lu, M. & Kou, S. (1989). Power input in gas metal arc welding of aluminum-Part 1. *Welding Journal*, Volume 68, Issue 9, pp. S382-S388, (Sep., 1989), ISSN 0043-2296
- Lu, M. J. & Kou, S. (1989). Power input in gas metal arc welding of aluminum-Part 2. *Welding Journal*, Volume 68, Issue 11, pp. 452s - 456s, ISSN 0043-2296
- Lundin, C.; Danko, J. & Swindeman, C. (1989). Fusion of a SiC reinforced aluminum alloy 2024, *Proceedings of ASME 1989 International Conference on Recent trends in welding science and technology*, pp. 303-307, ISBN ?, Gatlinburg, Tennessee, USA, May 14-18, 1989
- Malin, V. (1995). Study of metallurgical phenomena in the HAZ of 6061-T6 aluminium welded joints. *Welding Journal*, Vol.74, No.9, pp. 305s-18s, ISSN 0043-2296
- Miyazaki, M.; Nishio, K.; Katoh, M.; Mukae, S. & Kerr, H. (1990). Quantitative investigation of heat-affected zone cracking in aluminium alloy 6061. *Welding Journal*, Vol.69, Issue.9, pp.362s-71s, ISSN 0043-2296
- Moreira, P.; De Jesus, A.; Ribeiro, A. & Castro, P. (2008). Fatigue crack growth in friction stir welds of 6082-T6 and 6061-T6 aluminium alloys: as a comparison. *Theoretical and Applied Fracture Mechanics*, Vol. 50, Issue 2, (Oct 2008), pp. 81-91, ISSN 0167-8442
- Myhr, O.; Grong, O.; Fjaer, H. & Marioara, C. (2004). Modeling of the microstructure and strength evolution in Al-Mg-Si alloys during multistage thermal processing. *Acta Materialia*, Vol. 52, Issue 17, (Oct 2004), pp. 4997-5008, ISSN 1359-6454
- NACE MR0175/ISO 15156 (2009). Petroleum and natural gas industries - Materials for use in H₂S-containing environments in oil and gas production Part 1: General principles for selection of cracking-resistant materials
- Nandan, R.; DebRoy, T. & Bhadeshia H. (2008). Recent advances in friction-stir welding-process, weldment structure and properties. *Progress in Materials Science*, Vol. 53, Issue 6, (Aug 2008), pp. 980-1023, ISSN 0079-6425
- Natividad, C.; Salazar, M.; Espinoza-Medina, M.A. & Pérez, R (2007). A comparative study of the SSC resistance of a novel welding process IEA with SAW and MIG. *Materials Characterization*, Volume 58, Issue 8-9, (August-September 2007), pp. 786-793, ISSN 1044-5803
- Omweg, G.; Frankel, G.; Bruce, W.; Ramirez, J. & Koch G. (2003). Performance of welded high-strength low-alloy steels in sour environments. *Corrosion*, Volume 59, Issue 7, (July 2003), pp. 640-653, ISSN 0010-9312
- Ram, G.; Mitra, T.K.; Raju, M. & Sundaresan, S. (2000). Use of inoculants to refine weld solidification structure and improve weldability in type 2090 Al-Li alloy. *Materials Science and Engineering A*, Vol. 276, Issue 1-2, (Jan 2000), pp. 48-57, ISSN 0921-5093
- Rao, K.; Ramanaiyah, N. & Viswanathan, N. (2008). Partially melted zone cracking in AA6061 welds. *Materials & Design*, Vol. 29, Issue 1, (2008), pp 179-186, ISSN 0261-3069
- Seto, A.; Yoshida, Y. & Galtier, A. (2004). Fatigue properties of arc-welded lap joints with weld start and end points. *Fatigue & Fracture Engineering Materials & Structures*, Vol. 27, Issue 12, (Dec 2004), pp. 1147-115, ISSN: 8756-758X
- Turnbull, A. & Nimmo, B. (2005). Stress Corrosion Testing of Welded Supermartensitic stainless gas steel for oil and gas pipelines. *Corrosion Engineering Science and Technology*, Volume 40, Issue 2, (June 2005), pp. 103-109, ISSN 1478-422X

- Urena A.; Rodrigo P.; Gil L.; Escalera M. & Baldonado J. (2001). Interfacial reactions in an Al-Cu-Mg (2009)/SiCw composite during liquid processing - Part II - Arc welding. *Journal of materials science*, Vol. 36, Issue 2 (Jan 2001), pp. 429-439, ISSN: 0022-2461
- Urena, A.; Rodrigo, P.; Gil, L.; Escalera, M. & Baldonado, J. (2000). Interfacial reaction in Al-Cu-Mg (2009)/SiCP composite during liquid processing Part 1, *Journal of materials science*, Vol.32, pp. 419-428, ISBN 0022-2461

IntechOpen

IntechOpen



Arc Welding

Edited by Prof. Wladislav Sudnik

ISBN 978-953-307-642-3

Hard cover, 320 pages

Publisher InTech

Published online 16, December, 2011

Published in print edition December, 2011

Ever since the invention of arc technology in 1870s and its early use for welding lead during the manufacture of lead-acid batteries, advances in arc welding throughout the twentieth and twenty-first centuries have seen this form of processing applied to a range of industries and progress to become one of the most effective techniques in metals and alloys joining. The objective of this book is to introduce relatively established methodologies and techniques which have been studied, developed and applied in industries or researches. State-of-the-art development aimed at improving technologies will be presented covering topics such as weldability, technology, automation, modelling, and measurement. This book also seeks to provide effective solutions to various applications for engineers and researchers who are interested in arc material processing. This book is divided into 4 independent sections corresponding to recent advances in this field.

How to reference

In order to correctly reference this scholarly work, feel free to copy and paste the following:

Rafael García, Víctor-Hugo López, Constantino Natividad, Ricardo-Rafael Ambriz and Melchor Salazar (2011). Fusion Welding with Indirect Electric Arc, Arc Welding, Prof. Wladislav Sudnik (Ed.), ISBN: 978-953-307-642-3, InTech, Available from: <http://www.intechopen.com/books/arc-welding/fusion-welding-with-indirect-electric-arc>

INTECH
open science | open minds

InTech Europe

University Campus STeP Ri
Slavka Krautzeka 83/A
51000 Rijeka, Croatia
Phone: +385 (51) 770 447
Fax: +385 (51) 686 166
www.intechopen.com

InTech China

Unit 405, Office Block, Hotel Equatorial Shanghai
No.65, Yan An Road (West), Shanghai, 200040, China
中国上海市延安西路65号上海国际贵都大饭店办公楼405单元
Phone: +86-21-62489820
Fax: +86-21-62489821

© 2011 The Author(s). Licensee IntechOpen. This is an open access article distributed under the terms of the [Creative Commons Attribution 3.0 License](#), which permits unrestricted use, distribution, and reproduction in any medium, provided the original work is properly cited.

IntechOpen

IntechOpen